Doc Ophthalmol (2010) 120:273–289
DOI 10.1007/s10633-010-9231-4

ORIGINAL RESEARCH ARTICLE

Serial multifocal electroretinograms during long-term elevation and reduction of intraocular pressure in non-human primates

T. Michael Nork · Charlene B. Y. Kim · Gregg A. Heatley · Paul L. Kaufman · Mark J. Lucarelli · Leonard A. Levin · James N. Ver Hoeve

Received: 10 August 2009 / Accepted: 9 April 2010 / Published online: 27 April 2010

Abstract The purpose of this study was to evaluate the relationship between elevations of intraocular pressure (IOP) and the multifocal electroretinogram (mfERG) in non-human primates. Experimental glaucoma was induced in 4 rhesus and 4 cynomolgus monkeys by laser trabecular meshwork destruction (LTD) in one eye. To evaluate the contribution of ganglion cells to mfERG changes, one monkey of each species had previously underwent unilateral optic nerve transection (ONT). After ≥44 weeks of elevation, the IOP was reduced by trabeculectomy in 2 non-transected animals. In the intact (non-transected) animals, there was an increase in the amplitude of the early mfERG waveforms (N1 and P1) of the first-order kernel (K1) throughout the period of IOP elevation in all of the rhesus, but not all of the cynomolgus monkeys. A species difference was also present as a decrease of the second-order kernel, first slice (K2.1) in all of the cynomolgus monkeys but only in 1 of the rhesus monkeys (the 1 with the ONT). Similar IOP effects on the mfERG were seen in the ONT animals. Surgical lowering of IOP resulted in a return of the elevated K1 amplitudes to baseline levels. However, the depressed K2.1 RMS in the cynomolgus monkeys did not recover. These results demonstrate species-specific changes in cone-driven retinal function during periods of elevated IOP. These IOP-related effects can occur in the absence of retinal ganglion cells and may be reversible.

Keywords Experimental glaucoma · Multifocal electroretinogram · Optic nerve transection · Trabeculectomy

T. Michael Nork (✉) · C. B. Y. Kim · G. A. Heatley · P. L. Kaufman · M. J. Lucarelli · L. A. Levin · J. N. Ver Hoeve
Department of Ophthalmology and Visual Sciences, University of Wisconsin School of Medicine and Public Health, 600 Highland Ave. F4/336, Madison, WI 53792-3220, USA
e-mail: tmnork@wisc.edu

L. A. Levin
Department of Ophthalmology, University of Montreal, Montreal, QC, Canada

Introduction

Visual loss in glaucoma is commonly attributed to ganglion cell death with minimal preganglionic retinal involvement [1, 2]. However, there is an accumulating body of evidence that chronically elevated intra-ocular pressure (IOP) may also damage the outer retinal layers. Nork et al. [3] reported swelling of photoreceptor inner segments in a study of 128 human cadaveric eyes that were diagnosed with chronic open angle glaucoma. Recently Choi et al. [4] reported loss of cone signal in adaptive optics imaging in human patients with glaucoma. In a monkey model of glaucoma, cone swelling has also been reported [3]; however, cone loss has not been

found in this model [2, 3]. Both the Nork et al. [3] and Choi et al. [4] studies found that the glaucomatous effects on the outer retina were patchy, affecting some locations more than others. The patchy nature of damage to the outer retina in glaucoma makes it difficult to identify consistent anatomic changes.

At the biochemical level, Pelzel et al. [5] described alterations in the levels of opsin messenger RNA (mRNA) in glaucomatous eyes. Using opsin-specific probes, cone opsin mRNA was reduced both in a monkey model of chronic ocular hypertension and in humans with chronic glaucoma. The most affected region in the monkey was the mid-peripheral area, consistent with the typical field loss associated with human glaucoma as well as in behavioral studies of the monkey model [6–8]. Macular effects were also noted while the periphery was least involved.

Functional preganglionic retinal changes in glaucoma have been difficult to demonstrate. Several full-field electroretinogram (ffERG) studies are consistent with outer retinal effects in human glaucoma [9–13]. However, a thorough ffERG study by Holopigian et al. [14] found no electrophysiological evidence for diffuse photoreceptor abnormalities in primary open angle glaucoma in human patients. Similarly, no ffERG changes were evident in a monkey model of experimental glaucoma [15]. Weiner et al. [16] found that foveal cone focal ERG amplitude was subnormal in a significant proportion of human glaucomatous eyes. Eisner et al. [17, 18] observed decreased foveal flicker psychophysical sensitivity in elevated intraocular pressure and in early stages of glaucoma, which they interpreted as consistent with outer retinal dysfunction.

One of the challenges in establishing outer retinal effects in glaucoma is that, unlike the progressive, irreversible loss of ganglion cells, preganglionic cells such as cones and bipolars, do not typically die in large numbers, even in the face of considerable insult [1–3] and may even recover function. For example, photoreceptors tolerate hypoxia for extended periods, such as in the case of retinal detachment in patients whose photoreceptors may be completely separated from their choroidal blood supply for a week or more yet show remarkable recovery when the retina is re-attached [19, 20]. Even within non-human primates, there are subtle species differences in the nature of the corneal-derived measures of local retinal electrical activation [21] that preclude generalizing from a single non-human primate species to humans.

To study the effects of glaucoma on preganglionic retinal function and possible regional variation, we studied a well-characterized animal model of glaucoma in two species of macaque using the mfERG an electrophysiological measure, largely driven by preganglionic retina. We averaged numerous testing sessions in order to take into account the test–retest variability in mfERG responses, some of which may be due to the IOP fluctuations inherent in the LTD model. We also compared responses from the glaucomatous and control eye of each animal in order to account for day-to-day variations in the mfERG recordings, which seem to affect both eyes. Such inconsistency can be dealt with in part by averaging numerous testing sessions and by comparing the responses from the LTD and control eye of each animal.

To more precisely assess the role of preganglionic retina in this study, we recorded mfERGs in animals that first had unilateral optic nerve transection and then had IOP elevated by LTD. Finally, we assessed recovery of function in a subset of the LTD-only animals by lowering IOP with trabeculectomy.

Methods

Four rhesus (Macaca mulatta) and 4 cynomolgus (Macaca fascicularis) monkeys were used for the collection of data in this study. All of the experimental methods and techniques adhered to the ARVO Statement for the Use of Animals in Ophthalmic and Vision Research and were approved by our institution's animal care and use committee. The ages of the monkeys at the time the IOP was first elevated in the experimental eye to >25 mmHg were 7.0 ± 2.7 (mean $\pm$ standard deviation) years for the rhesus monkeys and 5.7 ± 0.7 years for the cynomolgus monkeys (Table 1).

Experimental glaucoma

Ocular hypertension was induced in all 8 animals by laser trabecular meshwork destruction [22–24]. A 532-nm diode laser and slit-lamp delivery system (OcuLight GL, Iridex Corp., Mountain View, CA) was employed to deliver laser light through a Kaufman-Wallow single mirror monkey gonioscopy contact lens (Ocular Instruments Inc., Bellevue, WA)

Table 1 Animal characteristics

Animal	Sex	Age (years) at first IOP > 25 mm Hg	Days of IOP > 25 mm Hg[a]	Mean IOP ± SD (mm Hg) OD[b]	Mean IOP ± SD (mm Hg) OS[c]	Number of mfERG tests with IOP > 25	% Axonal loss[d]
Rh1	F	6.3	1,402	38.2 ± 11.6	15.5 ± 2.9	30	80
Rh2	F	3.8	1,599	29.2 ± 9.1	16.4 ± 3.8	26	20
Rh3	M	10.2	406	47.0 ± 11.2	16.5 ± 2.5	17	50
Rh4[e]	M	7.7	1,329	42.1 ± 13.9	17.2 ± 3.0	41	100
Cy1	F	6.3	376	36.7 ± 10.6	13.2 ± 2.5	16	70[f]
Cy2	F	6.2	259	41.7 ± 7.5	13.2 ± 3.0	15	90
Cy3	M	5.5	308	24.2 ± 12.9	12.4 ± 3.2	17	80
Cy4[e]	M	4.8	369	49.3 ± 9.2	18.3 ± 3.2	7	100

[a] Days following first IOP measurement of greater than 25 mm Hg

[b] OD is the eye with experimental glaucoma

[c] OS is the control eye

[d] Approximate percentage loss of RGC axonal loss

[e] Underwent unilateral surgical transection of the optic nerve prior to elevation of IOP within the same eye

[f] May be an underestimate of RGC axonal loss due to tissue damage during preparation

applied to the cornea. Initially, approximately 130 confluent laser spots were delivered to the inferior 270° of the trabecular meshwork of the right eye. The spots were 75 μm in diameter, 1.0 W in strength and 0.5 s in duration and were directed to the anterior (non-pigmented) portion of the meshwork. Intraocular pressures were then checked at least weekly with a handheld digital tonometer (Tono-Pen XL; Mentor O & O, Nowell, MA). (This device underestimates the IOP at higher pressures in the cynomolgus monkey [25]. However, a similar study has not been done for the rhesus monkey.) If the IOP was not elevated in the treated eye after 3 weeks, a second laser treatment was performed that was also 270° and included the previously untreated superior trabecular meshwork. A third treatment was added 3 weeks later, if necessary. No animal required more than 3 treatments. Two of the rhesus monkeys (Rh1 and Rh2) had retinal laser spots (<5% of the total retina) placed in the peripheral retina of both eyes in a symmetrical manner as part of another study several months prior to inducing ocular hypertension. The laser spots were peripheral to Ring 1 and were encompassed by 3 of the 6 hexagons of Ring 2. The spots were placed symmetrically between the right and left eyes. (No differences were noted between Ring 1 and Ring 2 with respect to the retinal responses to experimental glaucoma).

Trabeculectomy

After many months of elevated IOP and repeated mfERG testing, 2 of the animals underwent successful IOP lowering (to a level of IOP consistently at or below that of the fellow eye). One trabeculectomy was performed on a rhesus (Rh3, with 406 days of IOP > 25 mm Hg, see Table 1), and 1 trabeculectomy was done on a cynomolgus (Cy3, with 308 days of IOP > 25 mm Hg). The method has been previously described in detail [26]. Briefly, following induction of general anesthesia, a superior limbal-based flap of conjunctiva and Tenon's was raised. Bleeding scleral blood vessels were cauterized. A pledget soaked with 0.4 mg/ml of mitomycin C was held against the exposed sclera for 5 min. After rinsing with a balanced saline solution, a half-thickness scleral flap was created. A Kelly Descemet punch was used to create a scleral ostomy, followed by a peripheral iridectomy. The scleral flap was closed with two nylon sutures at the corners, and the overlying conjunctiva was then closed with a single-layer running Vicryl suture.

Optic nerve transection

Two of the monkeys, 1 rhesus and 1 cynomolgus (Rh4 and Cy4, see Table 1) underwent optic nerve transection (ONT) in the right eye 140 days and

238 days, respectively, prior to the IOP being elevated above 25 mm Hg in the eye by LTD. The method used for ONT was described elsewhere [27]. Briefly, after induction of general anesthesia, a lateral orbitotomy with bone removal was created followed by a fornix-based peritomy and securing of the rectus muscles with 4-0 silk ties. The ties were used to rotate the eye such that the optic nerve could be identified. A length-wise incision was made in the optic nerve sheath. Once the nerve was exposed, it was cut with Westcott scissors 6 to 8 mm behind the globe, such that the cut was posterior to the entry of the retinal artery and vein. In addition to the 103-element mfERG testing presented here, these 2 animals also underwent 7-element mfERG and multifocal visual evoked potential measurements, the results of which were reported separately [28].

Electroretinography

The mfERG recording procedure was described in greater detail elsewhere [21]. Briefly, the animals were pre-anesthetized with ketamine (10 mg/kg, intramuscular (IM)). Deep anesthesia was induced by pentobarbital sodium, which suppressed eye movements. The induction dose of pentobarbital sodium was 15 mg/kg intravenous (IV) followed by supplemental doses of 10 mg/kg IV as needed to continue suppressing eye movement. Heart rate and blood oxygen saturation were monitored continuously with a pulse oximeter. Position was maintained with a bite-bar head holder. Wire specula were used for lid retraction. Pupillary mydriasis was produced by topical 1% tropicamide and 2.5% phenylephrine HCl. ERG-jet^{TM} contact lens electrodes were applied to the corneas with 2.5% hydroxypropyl methylcellulose. Reference electrodes for each eye consisted of subdermal needles that were placed on the ipsilateral outer canthus. VERIS Science^{TM} 4.1 (or 4.9) system (Electro-Diagnostic Imaging, Inc., San Mateo, CA) was applied for stimulus generation, data collection and preliminary analyses. The VERIS auto-calibration software/hardware system was applied for calibration of monitor (MGD403) stimulus luminance. Calibration procedures are carried out at the initiation of the study and whenever stimulus parameter modifications are implemented (on average, approximately monthly throughout the study). The visual stimulus consisted of 103 unstretched hexagonal elements that were displayed on a 21-inch Nortech Model UHR21L monochrome monitor (Nortech Imaging Technologies, Inc., Plymouth, MN, USA) or a Philips Model MGD403 monochromatic monitor (Koninklijke Philips Electronics NV, Eindhoven, The Netherlands). The VERIS fast m-sequence (binary maximum-length sequence cycle of 2^{14}-1) was employed with a frame rate of 75 Hz (13.3 ms per frame). Maximum and minimum luminances of the display were 200 cd/m^2 and $\sim$1 cd/m^2. Mean luminance was $\sim$100 cd/m^2. Sampling rate of the signal was 1,200 Hz (0.83 ms). The animals were positioned 20 cm from the monitor, and a +5 diopter lens was positioned in front of each eye. The eyes were unilaterally tested; an opaque occluder was situated in front of the untested eye during mfERG recordings. A reversing ophthalmoscope, which employed a corner cube reflector, was used to align the stimulus display with the visual axis. The visual angle subtended by the entire stimulus was 80°. Each hexagonal element subtended 8°. Testing order was counterbalanced, i.e., the eye tested first in any given session was the one tested second in the previous session.

Data analysis

Each 103-element first-order kernel (K1) trace array was visually inspected to locate the element with the largest N1-P1 amplitude. The trace array was grouped into four rings (Ring 1 [R1] through Ring 4 [R4]), which were concentric with the foveal stimulus element (R1, which is not strictly a ring but will be referred to as such for simplicity). Then, the processed data were exported for further analysis to a task-specific routine using MATLAB (The MathWorks, Inc., Natick, MA). FIR (finite impulse response) filters were used to separate frequencies greater or less than 80 Hz from the raw data waveforms. Data analysis was then performed either on the low-pass frequency components (LFC, less than 80 Hz) or the high frequency components (HFC, 80-120 Hz). Root-mean-square (RMS) determinations were also made for the 9-to-35 ms epoch of K1 for each of the 4 central rings (R1-4) and for the 0-to-80 ms epoch of K2.1 for R1-4. K1 response density amplitudes (RDAs or amplitudes) and implicit times (ITs, not interpolated) were derived from a peak-finding routine that was applied to the evoked potential ring averages to measure the first negative going peak (N1) and the first positive going peak (P1).

To evaluate the hypothesis that IOP elevation alters the mfERG, each animal's K1 and K2.1 measurements, collected across multiple tests during the period of IOP elevation (range 7–41), was submitted to separate ANOVAs using repeated-measures factors of Ring and Eye. These effects were evaluated using Greenhouse-Geiser corrections to the degrees of freedom for repeated measures. In addition, to correct for the effect of multiple tests across individuals, the significance levels for each major test (e.g., K1 RMS) were adjusted using the Bonferroni correction (alpha/N), where $N =$ the number of tests $\times$ number of animals. Thus, the alpha level of 0.05 was divided by 32, requiring a P of <0.00156 for a given test to reach significance.

Prior experience with similar data sets has shown considerable covariation between eyes in absolute amplitude across test sessions. To account for this correlation, the ratio between the right and left eye for each mfERG parameter was tested against the null hypothesis of a ratio of 1.0 using *t*-tests. A Bonferroni correction was applied in the evaluation of these tests.

To evaluate the null hypothesis that there is no species difference in mfERG response to elevated IOP, mixed-model ANOVAs were performed using the ratio of right and left eye mfERG measures (averaged across all test sessions for a given animal) for K1, K2.1 for LFC and HFC across the 4 central ring averages. Thus, the designs of these four separate ANOVAs include the between-subjects factor (Species) and the repeated-measures factor (Ring).

Histopathologic preparation of the optic nerves

All of the animals were killed with an overdose of pentobarbital followed by removal of the globes and fixation with 4% paraformaldehyde in 0.1 M sodium phosphate buffer adjusted to pH 7.6 for 24–72 h at 4°C and then placed in 0.1 M sodium phosphate buffer at 4°C for long-term storage.

Segments of the optic nerves of each eye were cut 2 mm posterior to the back of the globe. Each segment was approximately 2 mm in length. Shallow radial orientation cuts were made—a single cut at the 12 o'clock meridian and 2 parallel cuts on the nasal side. The optic nerve segments were then post-fixed in glutaraldehyde and embedded in Epon. Coronal sections of the nerves were then cut 1 μm thick, mounted on glass slides and stained with Richardson's stain. The optic nerve cross sections were examined by light microscopy. A semi-quantitative grading scheme based on that described by Chauhan et al. [29] was used for estimating axonal loss.

Results

Table 1 summarizes the animal characteristics. The duration of IOP elevation after the first measurement of greater than 25 mmHg varied from 259 to 1,599 days. As is typical of this model, the IOPs were variable and moderately high (means from 24.2 to 49.3 mmHg). From 7 to 41, mfERG testing sessions were performed on each animal during the epoch of elevated IOP. At the end of the study, histologic examination of the optic nerves revealed that the axonal loss was moderate to profound. No axons were visible in the optic nerves of the 2 animals that had ONT followed by experimental glaucoma.

Selected individual waveforms for the 2 recovery animals are shown in Fig. 1. These are the unfiltered waveforms from the single stimulus elements at the center of the 103 element field (Ring 1). The waveforms for the right and left eyes as well as the difference (OD-OS) waveform are superimposed. Each right–left pair of traces was obtained on the same test day. Similar, although not identical, traces were found for the right and left eyes at baseline (pre-IOP elevation) for both monkeys for K1 as well as K2.1. During the epoch of high IOP, elevated K1 amplitudes were evident in both Rh3 and Cy3. The K2.1 trace was only modestly affected in Rh3. However, K2.1 was clearly reduced in Cy3. After lowering of IOP by trabeculectomy, the K1 and K2.1 waveforms were nearly identical in the 2 eyes for Rh3. Recovery for Cy3 was limited to the earliest portion (N1 and the rising slope of P1) of K1. The later features (N2-P2) showed a phase shift that had a marked effect on the difference waveform. Following trabeculectomy, the K2.1 waveform of the experimental eye of Cy3 did not recover.

The largest K1 waveforms in both eyes were located in the central (macular) region as expected due to the unstretched stimulus pattern. Compared to the control eye, there was a marked increase in the amplitudes of the early waveform features in the glaucomatous eye that was particularly evident in the response to the central (macular) elements.

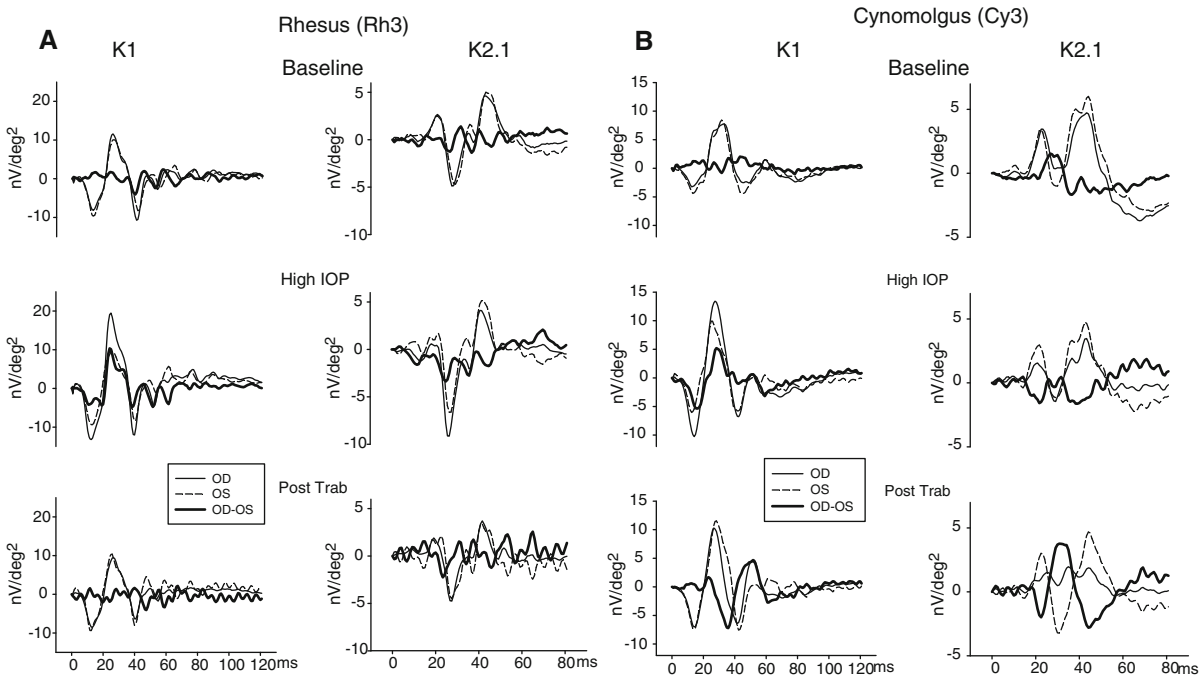

Fig. 1 Selected individual waveforms for the 2 recovery animals—Rh3 (**a**) and Cy3 (**b**). These are the unfiltered waveforms from single stimulus elements at or adjacent to the center (Ring 1) of the 103 element array. The waveforms for the right (*solid line*, high IOP) and left (*dashed line*, normal IOP) eyes as well as the difference (OD-OS, *bold line*) waveform are superimposed. Each right-left pair of traces was obtained on the same test day. The left column are the K1 waveforms and the right column the K2.1 waveforms. The upper plots are the baseline comparisons, the middle are during the epoch of elevated IOP and the lower are the waveforms post-trabeculectomy. See text for interpretation

Repeated-measures ANOVAs performed separately on each animal's K1 LFC RMS showed significantly higher amplitudes in the eye with experimentally elevated IOP as evidenced by Eye or Eye x Ring interactions. This pattern was present for all four rhesus and all four cynomolgus monkeys. A similar pattern was also evident in the K2.1 LFC RMS analyses. The K1 HFC RMS ANOVA Eye or Eye x Ring interactions were significant for 3 of 4 rhesus and 3 of 4 cynomolgus monkeys. The K2.1 HFC RMS ANOVA showed only 2 significant Eye × Ring interactions in the rhesus but all 4 cynomolgus monkeys showed significant effects involving eye for this measure. ANOVAs using N1 and P1 measures of mfERG amplitude showed patterns of effects to similar the RMS analyses.

As expected, there was a consistent significant interocular correlation of mfERG measures across testing sessions. To evaluate the consistency of direction of the difference, OD/OS ratios were calculated for each test session for each animal. *T*-tests (evaluated with Bonferroni correction) comparing the observed ratios versus the null hypothesis of 1.0 showed significant relative elevation of K1 RMS amplitudes for all for rhesus monkeys for each of the 4 ring averages. Only one of the cynomolgus monkeys showed consistent elevation of K1 LFC RMS amplitudes (Fig. 2a). The K2.1 LFC RMS amplitudes were elevated in one rhesus, depressed in another and unchanged in the other two. In contrast, all four cynomolgus monkeys' K2.1 LFC RMS were significantly lower than the expected ratio of 1.0 across all four ring averages (Fig. 2b).

Effects of IOP elevation on various specific waveform parameters were confirmed by repeated-measures *t*-tests comparing the experimental and fellow eyes. Two predominant effects of IOP elevation on the mfERG waveforms were evident. There was an increase in amplitude of the early mfERG waveforms (N1 and P1) of K1 in the rhesus monkeys and a decrease in K2.1 in the cynomolgus monkeys.

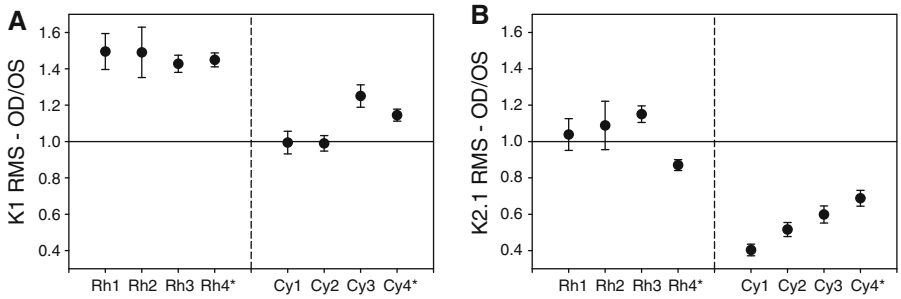

Fig. 2 **a** Comparisons of the K1 low frequency component RMS means and SEMs (over the 9–35 ms interval, Ring 2) of the OD/OS (experimental glaucoma/control eye) ratios for each animal. **b** Comparisons of the K2.1 (Ring 2 low frequency RMS values, 0-to-80 ms interval) response means and SEMs of the OD/OS (experimental glaucoma/control eye) ratios for each animal. * Underwent unilateral surgical transection of the optic nerve prior to elevation of IOP within the same eye

The difference in K1 OD/OS ratios for the rhesus N1-P1 is much greater that what we typically see for this species. We reviewed the data from 8 other control rhesus animals recorded for a separate study. The mean OD/OS ratio for Ring 2 of the K1 N1-P1 was 0.98 ± 0.127 (s.d.). The average OD/OS ratio for the 4 rhesus in this study was 1.47 during the epoch of elevated IOP. Thus, the experimental glaucoma animals have OD/OS ratios that were 3.7 standard deviations greater that the expected control value of 1.0—well above the 95% confidence interval of 1.96 standard deviations.

Both the increase in K1 RMS (9–35 ms) OD/OS ratio in the rhesus and the decrease in the K2.1 RMS (0–80 ms) ratio for in the cynomolgus monkeys were stable over the relatively long-time period of this study. Figure 3 shows the individual ratios versus days following IOP elevation to greater than 25 mmHg. In each case, the ratios were close to the mean even at the earliest test dates. In other words, the linear regression lines were essentially flat with a non-significant adjusted R^2 for the rhesus K1 of 0.005 and an adjusted R^2 for the cynomolgus K2.1 of 0.000.

A significant effect of species was evident in the OD/OS ratio analyzed with mixed-model ANOVAs based on the average ratio obtained across all sessions. The K1 LFC RMS ANOVA revealed significant effect of Species, [$F(1,6) = 65.3$, $P < 0.0001$] with no effect of Ring or Species × Ring interaction. The same Species effect held for K2.1 LFC RMS [$F(1,6) = 41.6$, $P < 0.001$] with no interaction with Ring. Similarly, an effect of Species was present in the K1 HFC RMS [$F(1,6) = 14.2$, $P < 0.01$, and K2.1 HFC RMS ($F(1,6) = 21.9$, $P < 0.01$] analyses.

The two monkeys that underwent ONT in the experimental eye prior to LTD showed effects on their waveforms similar to those seen in the monkeys with experimental glaucoma alone (Fig. 2). For

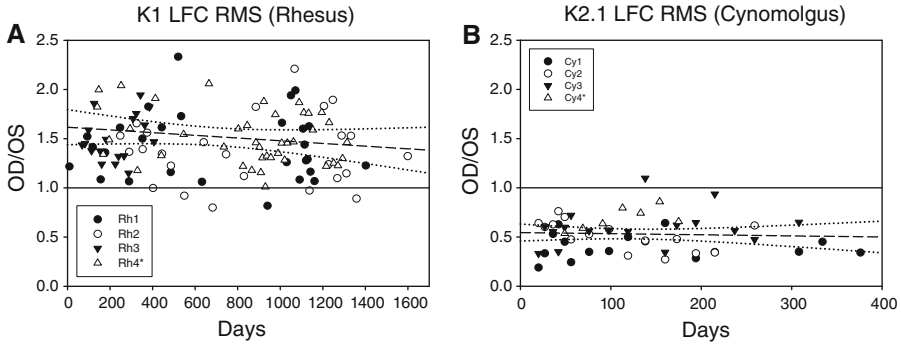

Fig. 3 Ratios of OD/OS (experimental glaucoma/control eye) at each test point for all animals plotted against days from the time that the IOP was first elevated above 25 mmHg in the experimental glaucoma eye. Linear regression lines (*dashed*) and 95% confidence limits (*dotted curves*) are shown. **a** K1 (Ring 2 low frequency component RMS over the 9–35 ms interval) of the 4 rhesus monkeys. **b** K2.1 (Ring 2 low frequency component RMS values, 0-to-80 ms interval) of the 4 cynomolgus monkeys

example, both of these animals had increased early (N1 and P1) K1 components, and the K2.1 was markedly reduced in the cynomolgus (CY4) compared to a K2.1 closer to baseline in the rhesus (Rh4).

Despite Eye × Ring interactions in many of the individual ANOVAs, no overall trend in the OD/OS ring ratios. There were no significant effects for Ring or Eye × Ring in the ANOVAs evaluating the effect of Species. Thus, there was no evidence for a consistent effect of retinal eccentricity in these data.

Recovery

One rhesus (Rh3) and one cynomolgus (Cy3) monkey underwent lowering of the intraocular pressure in the experimental eye by a trabeculectomy procedure. Figure 4 illustrates the IOP recordings of the treated (OD) and control (OS) eyes over the course of the experiment in the rhesus (Rh3). Superimposed on the IOP recordings are OD/OS ratios of the K1 low frequency component RMS for the 9 to 35 ms portion of the waveforms for Ring 2. Even with considerable test/retest variability, the mfERG amplitudes were correlated with experimentally elevated and reduced IOP. As shown in Fig. 4, the baseline (pre-IOP elevation) ratios (filled circles, prior to IOP elevation by LTD) varied around 1.0 (0.93 ± 0.10). Following 2 sessions of LTD (back arrows), the OD/OS ratios increased to 1.43 ± 0.05 (open circles). The ratios were relatively constant over this ensuing interval of elevated IOP. After 58 weeks of elevated IOP, a trabeculectomy was performed (gray arrow), after which, the IOPs in the experimental eye were lower than the fellow eye. At the 3 and 5 week test points following trabeculectomy, the OD/OS ratios remained high (1.51 and 1.46, respectively, black diamonds). However, from 7 weeks post-trabeculectomy onward, the ratios dropped back to nearly unity (1.06 ± 0.03). For both of the monkeys that underwent trabeculectomy, there was a strong correlation between IOP (IOP difference between OD and OS) versus K1 N1-P1 amplitude. The correlation coefficient for Rh3 was 0.62 (analysis of variance $P < 0.001$) and for Cy3, it was 0.54 (analysis of variance $P < 0.002$).

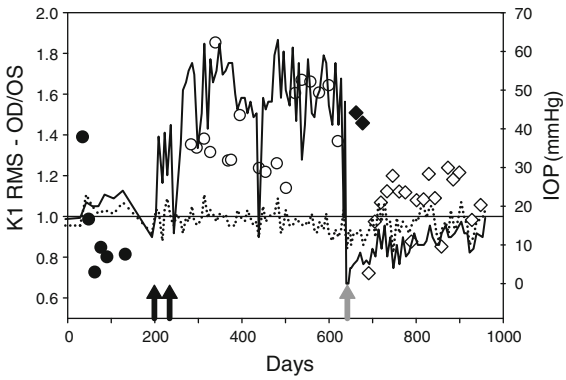

Fig. 4 IOP recordings (*right scale*) of the treated (*solid line*) and control (*dotted line*) eyes over the course of the experiment in Rh3. Superimposed on the IOP recordings are the OD/OS (experimental glaucoma/control eye) ratios of K1 RMS (Ring 2, 0–80 ms, low frequency component; discrete symbols). The *filled circles* show the OD/OS ratios prior to LTD (timing of the 2 sessions of LTD is indicated by the *black arrows*). The *open circles* are the OD/OS ratios during the epoch of elevated IOP. Following trabeculectomy (*gray arrow*), the OD/OS ratios initially were similar to pre-trabeculectomy (*filled diamonds*), but after 7 weeks approached baseline levels (*open diamonds*)

Means and standard errors of the means (SEMs) of K1 RMS (9-35 ms, low frequency component) and K2.1 RMS (0–80 ms, low frequency component) of Ring 2 for Rh3 and Cy3 for the 3 epochs (baseline, high IOP and post-trabeculectomy) are shown in Fig. 5. The means were fairly constant over time for all parameters of the control eyes (black dots). However, changes were evident in many of the parameters of the experimentally glaucomatous eyes. K1 was markedly increased during the period of high IOP for both Rh3 and Cy3. Following trabeculectomy, the mean K1 returned to levels similar to the control eyes in both monkeys (Fig. 5a). The K2.1 response differed markedly between the two animals. Rh3 showed a mild increase in K2.1 during the epoch of high IOP and then a moderate reduction following IOP lowering by trabeculectomy. Cy3, by comparison, showed a marked decrease in K2.1 with high IOP. There was no recovery of the waveform after IOP lowering. The mean K2.1 after IOP lowering was even less than during the time of high IOP (Fig. 5b).

Discussion

Increased N1-P1Amplitude

A striking effect of experimental glaucoma on the mfERG that we observed was an increase in the early waveform features of the K1 response (RMS and N1

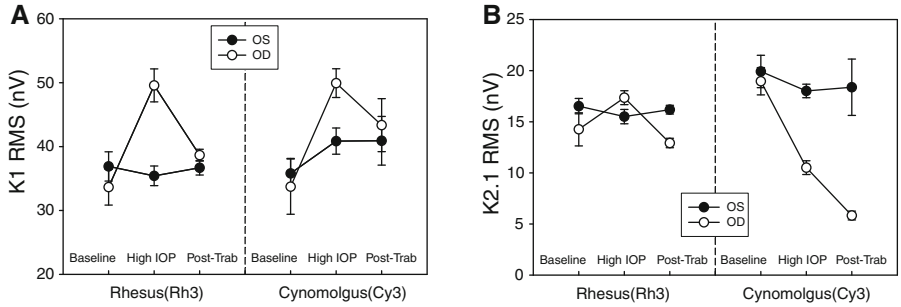

Fig. 5 Means and SEMs of the K1 RMS (9–35 ms, low frequency component) (**a**) and K2.1 RMS (0–80 ms, low frequency component) (**b**) of Ring 2 for Rh3 and Cy3 for the 3 epochs (*baseline*, high IOP and post-trabeculectomy)

and P1) in all 4 of the rhesus monkeys. An increase in N1-P1 was reported by Frishman et al. [30] in rhesus monkeys and Hare et al. [31] in cynomolgus monkeys. (Although we saw an N1-P1 increase in only 2 of the 4 cynomolgus monkeys in this study.) Both groups attribute the phenomenon to removal of the inner retinal components that might be otherwise inhibiting the earlier waves. Consistent with this hypothesis is the similar increase in early waveforms found following intravitreous injections of the voltage-sensitive sodium channel blocker tetrodotoxin (TTX) [30, 32, 33].

Although removal of the inner retinal contributions might explain part of the increased amplitude seen in experimental glaucoma, a contributing factor could be preganglionic injury. Supranormal (also known as hyperabnormal or supernormal) ffERG has been reported in a variety of outer retinal injuries and diseases in humans [34]. Feigl et al. [35] described increased N1-P1 mfERG amplitudes in human patients with multiple evanescent white dot syndrome (MEWDS) within 1 to 7 days of the onset of symptoms. However, the waveforms decreased to normal or subnormal values 2 weeks later. Increased K1 mfERG amplitudes were also observed immediately after prostaglandin E_1 infusion in some, but not all, patients with dry age-related macular degeneration [36]. In monkeys, supranormal mfERG effects have been reported to occur within a few minutes following laser grid photocoagulation to the retina (Brown, J. et al. *IOVS* 2004;45: ARVO E-abstract 2029 and Ver Hoeve, J. N. et al. *IOVS* 2004;45: ARVO E-abstract 4239).

Adachi-Usami et al. [37] found a transient increase of both the a- and b-wave in mice that were injected with 40 mg/kg of the RPE toxin, sodium iodate, through the caudal vein. One day after injection, the ffERG maximal a- and b-waves were markedly increased compared to baseline. However, the b-wave threshold intensity also increased and the implicit time of the b-wave increased, as well. Two days post injection, the ffERG was markedly reduced. Electron microscopy done 1 day post injection showed granular electron dense deposits and vacuolization of the retinal pigment epithelium as well as dilated outer segment disks, which they interpreted as indicating an early stage of degeneration. Ultrastructural defects became marked at 2 days and 4 days post injection. Adachi-Usami et al. [37] proposed that changes in gain between the receptor response and the response of the downstream cells could be a factor in their ffERG results. This effect, early on, might overwhelm an apparent decrease in the efficiency of photon capture (as evidenced by the decreased sensitivity). Supranormality in that study was found in both the a- and b-wave responses, suggesting that down-stream cells (e.g., bipolar cells and/or Müller cells) were affected as well as the photoreceptors.

The origins of the mfERG waveforms have not been as extensively studied as the ffERG. Work by Hood et al. [38] in rhesus monkey indicates that much of the N1-P1 portion may be attributable to responses of the bipolar cells (although the photoreceptors make some contribution—especially to N1 in the central macula). Thus, abnormalities in N1-P1 could indicate either photoreceptor or bipolar injury. In any event, loss of retinal ganglion cells would not be expected to have a major influence on N1-P1.

Outer retinal involvement (all cell types other than RGCs) could explain several aspects of our observations. First, the N1-P1 increase occurred immediately upon IOP elevation. So, it must not be the result of missing RGCs, which require 2 or 3 months to degenerate, even after optic nerve transection. [39]. Second, the increase in N1-P1 was constant over

many months of elevated IOP (see Fig. 3). If this was a response to RGC death, we would expect it to become more prominent over time. Third, the N1-P1 waveforms returned to pre-IOP levels in 2 of the animals (Rh3 and Cy3); the supranormal effect was returned to nearly normal levels after 406 and 308 days (respectively) following trabeculectomy. In the case of the rhesus monkey (Rh3), 50% of the ganglion cells had died, and 80% had died in the cynomolgus monkey (Cy3). If the N1-P1 increase was the result of loss of RGC activity, we would expect at best only partial recovery in these animals. It is also relevant that the K1 N1-P1 increase was not found in all of the monkeys. We saw no N1-P1 elevation in 2 of the cynomolgus monkeys despite the fact that their pressure profiles and RGC losses were similar to the animals that had increased N1-P1 waveforms. Taken together with the previously described morphologic and biochemical changes in the cones, we believe that the observed K1 changes could be explained by outer retinal injury. By contrast, the K2.1 decrement in the cynomolgus monkeys appeared to be permanent and, thus, could be the result of RGC functional loss.

Despite supranormality in the ffERG a- and b-waves following sodium iodate injection, Adachi-Usami et al. [37] found that there is an increase in b-wave implicit time, which they concluded was another indicator of outer retinal injury. In a likely parallel, we observed that both the N1 and P1 mfERG implicit times were characteristically increased in those animals that had supranormal N1-P1 complexes.

The number of animals in this study is too small to make definitive conclusions regarding species differences in the supranormal response of N1-P1 to chronically elevated IOP. However, there appeared to be a trend toward more consistent K1 N1-P1 supranormality among the rhesus. All 3 of the non-ONT rhesus showed exaggerated N1-P1 waveforms, whereas only 1 of the 3 cynomolgus monkeys demonstrated a similar effect. Even so, Hare et al. [31] found supranormality using only cynomolgus animals with long-term, high IOP experimental glaucoma.

Decrease in the second-order kernel

A more consistent species-specific effect was observed for K2.1. The K2.1 waveforms in the experimentally glaucomatous eyes (including the OHT/ONT eye) were markedly reduced in all 4 of the cynomolgus monkeys (Fig. 2b). However, no clear trend was evident for the 4 rhesus monkeys. To our knowledge, there has been no previous report of a direct comparison of the relative effect of experimental glaucoma on K2.1 in these two species utilizing the same stimulus parameters. Even so, there have been several studies on cynomolgus monkeys alone showing a marked reduction in K2.1 using a similar mfERG stimulus to the one that we employed (Raz D et al. *IOVS* 2003;44: ARVO E-abstract 4117) [31, 40, 41].

The only published study of the effect of experimental glaucoma in rhesus monkeys using the same fast m-sequence mfERG was done by Frishman et al. [30]. They induced experimental glaucoma in 5 rhesus monkeys and compared their results to the control eyes and to the effect of injecting TTX and N-methyl-D-aspartate (NMDA) into the vitreous. TTX blocks the spiking action potentials of the retinal ganglion and amacrine cells. NMDA causes excitotoxic damage to retinal ganglion cells when injected intravitreally. Indeed, an increase in the K1 and decrease in K2.1 amplitude in both experimental glaucoma and following TTX/NMDA injection was found by these investigators.

The K1 amplitude results of the present study agree with those of Frishman et al. [30] in that we found marked increases in K1 in all 4 of our rhesus monkeys. However, the K2.1 mfERG was not consistently decreased. Indeed, there was a trend toward an increase in the 3 rhesus with experimental glaucoma alone. Only Rh4 that had ONT followed by experimental glaucoma showed decreased K2.1. Even so, the decrease in K2.1 was modest in this animal compared to the 4 cynomolgus monkeys (Fig. 2b). One possible explanation for this discrepancy might be that more ganglion cells were killed by experimental glaucoma in their animals (and in our ONT animal) than in our 3 rhesus monkeys. However, they did not provide an estimate of the number of ganglion cells surviving in their animals. In our case, there was no obvious association between the amount of ganglion cell loss and K2.1 depression. Another possible explanation for the difference in waveforms between our study and Frishman et al. [30] might be the type of anesthetic. A ketamine/xylazine combination was used in the Frishman study while we used pentobarbital. Ketamine works mainly

through blockade of the N-methyl-d-aspartate (NMDA) glutamate receptors [42, 43] whereas pentobarbital works mainly by binding to the γ-aminobutyric acid ($GABA_A$) receptors [44]. Although we have not used ketamine/xylazine alone, we have found differences in the waveforms between pentobarbital and propofol anesthetics (Kim, C.B.Y. et al. *IOVS* 2010;51:ARVO E-abstract 1079).

Fortune et al. [45] investigated the effects of ganglion cell death caused by anterior optic nerve ischemia from chronic infusion of endothelin-1. They found little difference in either the K1 or the K2.1 components despite the presence of moderate ganglion cell loss in their model. A possible explanation for this is that, although their model affects circulation around the optic nerve, it may not completely replicate the decrease in choroidal circulation that is associated with elevated intraocular pressure. Another possibility is that the mfERG recordings were made at some point after completion of the endothelin-1 infusion, thus any outer retinal effects might have recovered.

Species differences

The mechanism explaining why rhesus and cynomolgus monkeys should exhibit different mfERG responses to experimental glaucoma is not clear. Comparisons between distantly related vertebrate species have found many similarities in the distributions of the major neurotransmitters and their receptors. Vardi et al. [46] found that monkey, cat and rabbit express the same isoform of the mGluR6 receptor in all 5 types of ON bipolar cells. In an earlier study, Mosinger et al. [47] observed that the distribution of GABA-like immunoreactivity was similar in various mammalian and non-mammalian species. Koulen et al. [48] compared the distribution of $GABA_A$ and glycine receptors (especially in the bipolar cells) of rats and rabbits, again finding no apparent differences. However, some species differences have been documented, such as the distribution of $GABA_A$ receptors in goldfish and chickens [49]. Among primates, there seems to be less obvious variation. For example, Vardi and Sterling [50] found no difference in the subcellular localization of $GABA_A$ receptor on bipolar cells in cynomolgus and human retina.

Perhaps more enlightening are 2 physiologic studies comparing differential species responses in Müller cells. In the first, Chao et al. [51] performed morphological and electrophysiological (in vitro whole-cell voltage clamp) studies in 22 mammalian species. They concluded that specific metabolic activities of Müller cells must differ greatly between species. In the second study, Pannicke et al. [52] compared the physiological properties of Müller cells from cynomolgus monkeys and human retinas in vitro. They noted that, although the basic membrane properties are very similar between cynomolgus monkey and human Müller cells, there were also important differences, such as a lack of $GABA_A$ receptors and of CA^{2+}-dependent K^+ currents in monkey cells. Indeed, the differences sufficiently great enough for them to conclude that, "in general, monkey cells are no more similar to human cells than those from standard laboratory animals" [52]. We are not aware of such physiologic studies comparing the in vitro responses of rhesus and cynomolgus monkeys. However, Kim et al. [21] described not only species but also gender differences in the mfERG waveforms between these 2 species. Given such differences, we believe that it is inappropriate to combined data across species for statistical purposes.

A possible explanation for the differences in mfERG response of rhesus and cynomolgus monkeys to experimental glaucoma might a species difference in cellular susceptibility to excitotoxic injury that may result from elevated IOP. Luo et al. [53] observed that cultured adult pig RGCs responded differently that either adult or newborn rat cultured RGCs when exposed to NMDA and glutamate. Alternatively, it could be that the mfERG waveforms (which are an integration of the contributions from many retinal cell types) in the rhesus and cynomolgus monkeys have different origins. For example, the RGCs might contribute a greater portion of the K2.1 in the cynomolgus monkey than they do in the rhesus monkey.

One can only speculate at this time whether the rhesus or the cynomolgus monkey is a better model for human glaucoma. However, elevated N1P1 waveforms have been reported in other human diseases [35] (Nork et al. *Trans Am Ophthalmol Soc* 2004;102:266 abstract). Furthermore, the effect of human glaucoma on the K2.1 is far less dramatic that what we found with our cynomolgus monkeys. So, the rhesus monkey may prove to be a somewhat better model of human glaucoma with respect to the mfERG.

Variability

A long-term repeated-measures study provides information on measurement variability of mfERG testing. Although there were individual differences in amplitudes, there was also a strong test day effect (data not shown). That is, the animals seemed to have days in which the signal strength for both eyes was strong or weak relative to the average. The reasons for such day-to-day effects are unknown but might include anesthesia level, small variations in contact lens or reference electrode placement and environmental electrical noise. In addition, some animals simply have larger and more consistent baseline waveforms than others. Both of these types of variability can be partly compensated for by comparing ratios of the responses of the experimental and control eyes in the same animal on the same test day. Note that the order of testing treated and untreated eyes was alternated between each session and therefore balanced across the study, which is critical in these types of investigations. Figure 2 shows a similarity among the 4 rhesus monkeys for the OD/OS ratio of the K1 RMS. Only with a large number of mfERG data points are trends in IOP and recovery effects evident within the variations due to test day and individuals fully evident. Individual differences were particularly noticeable in the K1 RMS (9–35 ms) of the cynomolgus monkeys. Whether this effect is due to species/gender [21] or simply individual idiosyncratic responses cannot be determined definitively with only 8 animals. However, the depression in K2.1 RMS (0–80 ms) was pronounced in all 4 of the cynomolgus monkeys and yet only seen (to a lesser degree) in the one rhesus that also had an ONT. We conclude that there is a strong species-dependent effect of IOP on the K2.1 RMS (0–80 ms).

Recently, Kremers et al. [54] reported the results of a study of experimental glaucoma in cynomolgus monkeys in which numerous tests were performed during the period of elevated IOP. Unlike our study, they summed the absolute differences at each signal data point during the 0 to 90 ms interval of K1; no information was obtained regarding the individual wave features (e.g., N1 and P1) or the K2.1. Furthermore, because they looked only at absolute differences, any supranormal effects could not be ascertained. However, they did find that there were significant differences that persisted throughout the testing period for some, but not all of the animals. They also observed that the test–retest variability was reduced by comparing experimental (OD) to control (OS) eyes over time versus comparison with the baseline recordings in the same eye.

Shape of waveforms

The waveforms recorded in our experiment have shapes that, while consistent with those found by some investigators [31, 33, 40, 41, 45, 55], differ from recordings by other groups [30, 32] who observed larger-amplitudes of the higher frequency components than we report here. Reduced high frequency components have been reportedly due to the use of a 60-Hz notch filter (although we did not use a filter), species differences, electrode type, electrode placement and/or anesthetic protocol [31, 33]. Careful investigation of species/gender differences [21] and electrode placement [56] has confirmed that these can affect the mfERG waveforms. However, species differences between normotensive rhesus and cynomolgus are small an unlikely to account for the large changes observed in this study (e.g., compare the baseline waveforms in Fig. 1a and b).

Effect of ONT

The 2 animals (Rh4 and Cy4) with both ONT and experimental glaucoma showed effects on the mfERG that were similar to experimental glaucoma alone. Adding ONT to the experimental glaucoma is a means of removing all the retinal ganglion cells (Table 1) and, therefore, eliminating any possible ganglion cell contribution from the measured effects. Thus, the observed effects, such as K1 increase, are not likely caused by the surviving ganglion cells.

HFC contribution

In the full-field ERG, the high-frequency components of the waveforms (the oscillatory potentials) are thought to be post-receptoral in origin—perhaps arising from the vicinity of the inner plexiform layer [57, 58]. Weak high-frequency components have been observed in the fast-sequence mfERG used in this study. However, a slowed m-sequence, in which several blank frames are inserted between flashes, results in more prominent mfERG oscillatory

potentials (HFCs) [59]. Various studies, including a recent report of marked reduction in the mfERG HFCs in rhesus monkeys that underwent ONT [60] and in experimental glaucoma in rhesus monkeys [61, 62], suggest that the HFCs in the slow-sequence mfERG may have their origin, at least in part, in the ganglion cells. Nevertheless, we were able to obtain HFC responses using the fast-sequence mfERG that, when averaged over multiple recording sessions, were statistically different from the fellow (control) eyes. A consistent decrement associated with axonal loss was not observed. Instead, the general pattern of HFC changes was similar to those found for the LFCs–namely, increased K1 responses for the 4 rhesus monkeys and decreased K2.1 responses for the cynomolgus animals (data not shown).

An increase in K1 HFC amplitude is in the opposite direction of results reported by Frishman et al. [30], who found that the HFC peak at 75 Hz present in the normal fast-sequence mfERG power spectrum was markedly depressed in rhesus monkeys with advanced experimental glaucoma. A number of differences exist between their experimental setup and ours; including the severity of experimental glaucoma, type of anesthesia, recording electrode and the size of the mfERG stimulus elements. The mfERG waveforms are known to be affected by anesthesia (Kim, C.B.Y. et al. *IOVS* 2010;51: ARVO E-abstract 1079), electrode type [63] and electrode montage [56]. It may be that due to one or a combination of these factors our mfERG waveforms have more outer retinal (non-ganglion cell) contribution at the higher frequencies. However, for one of these methodological factors to account for the direction of effects, the effect of experimental glaucoma on the retinal neurons responsible for HFC would have to be altered radically by one or more of these factors, for example pentobarbital versus ketamine/xylazine.

Perhaps a more likely reason for the apparent discrepancy is that the analyses used in this study considered K1 HFCs as the RMS amplitude between 80 and 120 Hz within the 9-to-35 ms epoch of the K1 waveform. The Frishman et al. [30] study performed a fast Fourier transform (FFT) on the entire 75 ms K1 waveform. Thus, the present study found that HFCs increase (relative to the fellow control eye) within an early portion of the K1 waveform, suggesting that early HFCs may be modulated by glaucoma differently that later-occurring HFCs. Some decrease in the later-occurring HFCs is also apparent as ripples in the difference waveform in K1 waveforms in the present study, as shown the middle panel of Fig. 1a.

Temporal effects and reversibility

One of the most prominent changes, increase in the N1-P1 complex of K1 in the rhesus monkeys occurred rapidly (at the time of the first measurement with high IOP) and persisted in all of the animals for the entire period of elevated IOP. There was no statistically significant degradation of the increase with time (Fig. 3a). Likewise, the marked decrease in the K2.1 in the cynomolgus monkeys happened soon after the IOP became elevated and persisted throughout the period of elevated IOP (Fig. 3b).

In 2 of the animals (Rh3 and Cy3), we performed a trabeculectomy after 406 and 308 days, respectively. This brought the IOP in the experimental eyes to near or below the fellow eye in each animal. Both animals showed a return of the K1 N1-P1 to nearly normal levels. However, the K2.1 that had been markedly decreased in Cy3 did not recover (Fig. 5).

IOPs varied markedly from measurement-to-measurement (see Fig. 4), as is typical for this animal model. However, there was no obvious correlation between these short-term fluctuations in IOP and the N1-P1 increase. One possible reason is that although increase occurs rapidly after IOP elevation, recovery takes time. Figure 4 shows that the increased N1-P1 persisted for at least 5 weeks after the IOP was surgically lowered before it approached baseline levels.

Taken together, these findings could be explained by preganglionic retinal (including photoreceptor, bipolar, Müller, horizontal or amacrine cell) effects of experimental glaucoma. Retinal ganglion cells are susceptible to prolonged periods of elevated IOP, probably because of axonal damage at the optic nerve head. In contrast, the other retinal cells are relatively resistant. Although photoreceptor loss has been documented in humans in 2 independent studies [3, 64], such loss remains controversial [1, 2]. We are unaware of any studies showing a similar loss of photoreceptors in experimental glaucoma in monkeys. Even the displaced amacrine cells located in the retinal ganglion cell layer are spared in experimental glaucoma [15]. In other words, the pathologic

changes seen in the outer retina may, for the most part, represent injury but not necessarily permanent damage. Since the pre-ganglionic retinal cells are relatively resistant to irreversible damage (i.e., cell death) except for cases in which the IOP is very high. Thus, reversibility with IOP lowering could be explained by functional recovery of these pre-ganglionic cells. Considering that in Rh3, 50% of the RGCs had died and 80% had died in Cy3, it is unlikely that what appears to be nearly full recovery of K1 N1-P1 would be attributable to the few remaining RGCs. This contrasts with the irreversibility of the K2.1, which is more consistent with permanent injury to retinal ganglion cells.

Regional effects

Significant Eye × Ring interaction was observed for 45 of the 64 ANOVAs. However, when OD/OS ratios were plotted by ring, there did not appear to be an obvious trend. That is, some animals for some parameters showed a greater effect in the central rings, while others had most of the effect in the peripheral rings (data not shown). No animal exhibited a clearly mid-peripheral area of either decreased or increased amplitude. While the Eye × Ring interactions and a lack of regional effect in the OD/OS ratios might seem to be a contradiction, they actually are not in disagreement. Because of the use of unstretched stimuli, both the K1 and K2.1 waveforms are most pronounced in Ring 1 and become weaker with increasing Ring number. So, any effect that is proportional (constant ratio) across rings would have the greatest numerical (subtractive) difference in Ring 1—thus, the Eye × Ring effect.

Experimental glaucoma in monkeys has been shown to share an important feature with human glaucoma. Behavioral studies in monkeys by Harwerth et al. [6–8] have determined that the visual field losses tend to be uneven or patchy and vary from individual to individual. In general, there is a tendency for the greatest field losses to occur in the mid-peripheral zone. Even so, it has been well established in humans with glaucoma [65–69] as well as monkeys with experimental glaucoma [15, 70–72] that the ganglion cell loss is spread throughout the retina and is certainly evident in the central macula as well as in the periphery. It has been proposed that there is enough redundancy in the macular portion of the visual system such that the central field is relatively less sensitive to ganglion cell loss than in the periphery [65, 72].

To the extent that we found regional and individual variability and that the macular electrical function was affected at least as much as the in the periphery, our results are broadly consistent with the ganglion cell losses known to occur in glaucoma.

Summary

Numerous alterations of mfERG waveforms are seen in response to long-term experimental IOP elevation in non-human primates—some of which appear to be species specific. These results demonstrate that changes in cone-driven retinal function during periods of elevated IOP can occur in the absence of retinal ganglion cells and that these changes may be reversible.

Acknowledgments The authors thank Carrie Bunger, Beth Hennes, and Cassandra Miller for providing technical assistance. *Support*: R01 EY014041 (Dr Nork), National Institutes of Health (NIH); R01-EY02698 (Dr. Kaufman), NIH; P30 EY016665 (Drs. Nork and Kaufman), NIH; the American Health Assistance Foundation; the Retina Research Foundation, Walter H. Helmerich Chair (Dr Nork); and Research to Prevent Blindness.

References

1. Kendell KR, Quigley HA, Kerrigan LA, Pease ME, Quigley EN (1995) Primary open-angle glaucoma is not associated with photoreceptor loss. Invest Ophthalmol Vis Sci 36:200–205
2. Wygnanski T, Desatnik H, Quigley HA, Glovinsky Y (1995) Comparison of ganglion cell loss and cone loss in experimental glaucoma. Am J Ophthalmol 120:184–189
3. Nork TM, Ver Hoeve JN, Poulsen GL, Nickells RW, Davis MD, Weber AJ, Vaegan SarksSH, Lemley HL, Millecchia LL (2000) Swelling and loss of photoreceptors in chronic human and experimental glaucomas. Arch Ophthalmol 118:235–245
4. Choi SS, Zawadzki RJ, Keltner JL, Werner JS (2008) Changes in cellular structures revealed by ultra-high resolution retinal imaging in optic neuropathies. Invest Ophthalmol Vis Sci 49:2103–2119
5. Pelzel HR, Schlamp CL, Poulsen GL, Ver Hoeve JA, Nork TM, Nickells RW (2006) Decrease of cone opsin mRNA in experimental ocular hypertension. Mol Vis 12:1272–1282
6. Harwerth RS, Smith EL 3rd, DeSantis L (1997) Experimental glaucoma: perimetric field defects and intraocular pressure. J Glaucoma 6:390–401
7. Harwerth RS, Carter-Dawson L, Shen F, Smith EL 3rd, Crawford ML (1999) Ganglion cell losses underlying

visual field defects from experimental glaucoma. Invest Ophthalmol Vis Sci 40:2242–2250
8. Harwerth RS, Crawford ML, Frishman LJ, Viswanathan S, Smith EL 3rd, Carter-Dawson L (2002) Visual field defects and neural losses from experimental glaucoma. Prog Retin Eye Res 21:91–125
9. Alvis DL (1966) Electroretinographic changes in controlled chronic open-angle glaucoma. Am J Ophthalmol 61:121–131
10. Fazio DT, Heckenlively JR, Martin DA, Christensen RE (1986) The electroretinogram in advanced open-angle glaucoma. Doc Ophthalmol 63:45–54
11. Holopigian K, Seiple W, Mayron C, Koty R, Lorenzo M (1990) Electrophysiological and psychophysical flicker sensitivity in patients with primary open-angle glaucoma and ocular hypertension. Investigative Ophthalmology & Visual Science 31:1863–1868
12. Odom JV, Feghali JG, Jin JC, Weinstein GW (1990) Visual function deficits in glaucoma. Electroretinogram pattern and luminance nonlinearities. Arch Ophthal 108:222–227
13. Vaegan GrahamSL, Goldberg I, Buckland L, Hollows FC (1995) Flash and pattern electroretinogram changes with optic atrophy and glaucoma. Exp Eye Res 60:697–706
14. Holopigian K, Greenstein VC, Seiple W, Hood DC, Ritch R (2000) Electrophysiologic assessment of photoreceptor function in patients with primary open-angle glaucoma. J Glaucoma 9:163–168
15. Frishman LJ, Shen FF, Du L, Robson JG, Harwerth RS, Smith EL 3rd, Carter-Dawson L, Crawford ML (1996) The scotopic electroretinogram of macaque after retinal ganglion cell loss from experimental glaucoma. Invest Ophthalmol Vis Sci 37:125–141
16. Weiner A, Ripkin DJ, Patel S, Kaufman SR, Kohn HD, Weidenthal DT (1998) Foveal dysfunction and central visual field loss in glaucoma. Arch Ophthalmol 116:1169–1174
17. Eisner A, Samples JR, Campbell HM, Cioffi GA (1995) Foveal adaptation abnormalities in early glaucoma. J Opt Soc Am A Opt Image Sci Vis 12:2318–2328
18. Eisner A, Samples JR (2000) Flicker sensitivity and cardiovascular function in healthy middle-aged people. Arch Ophthalmol 118:1049–1055
19. Burton TC (1982) Recovery of visual acuity after retinal detachment involving the macula. Trans Am Ophthalmol Soc 80:475–497
20. Diederen RM, La Heij EC, Kessels AG, Goezinne F, Liem AT, Hendrikse F (2007) Scleral buckling surgery after macula-off retinal detachment: worse visual outcome after more than 6 days. Ophthalmology 114:705–709
21. Kim CB, Ver Hoeve JN, Kaufman PL, Nork TM (2004) Interspecies and gender differences in multifocal electroretinograms of cynomolgus and rhesus macaques. Doc Ophthalmol 109:73–86
22. Gaasterland D, Kupfer C (1974) Experimental glaucoma in the rhesus monkey. Invest Ophthalmol 13:455–457
23. Quigley HA, Hohman RM (1983) Laser energy levels for trabecular meshwork damage in the primate eye. Investigative Ophthalmology & Visual Science 24:1305–1307
24. Nork TM, Poulsen GL, Nickells RW, Ver Hoeve JN, Cho NC, Levin LA, Lucarelli MJ (2000) Protection of ganglion cells in experimental glaucoma by retinal laser photocoagulation. Arch Ophthalmol 118:1242–1250
25. Peterson JA, Kiland JA, Croft MA, Kaufman PL (1996) Intraocular pressure measurement in cynomolgus monkeys. Tono-Pen versus manometry. Invest Ophthalmol Vis Sci 37:1197–1199
26. Heatley G, Kiland J, Faha B, Seeman J, Schlamp CL, Dawson DG, Gleiser J, Maneval D, Kaufman PL, Nickells RW (2004) Gene therapy using p21WAF-1/Cip-1 to modulate wound healing after glaucoma trabeculectomy surgery in a primate model of ocular hypertension. Gene Ther 11:949–955
27. Gonnering RS, Dortzbach RK, Erickson KA, Kaufman PL (1984) The cynomolgus monkey as a model for orbital research. II. Anatomic effects of lateral orbitotomy. Curr Eye Res 3:541–555
28. Maertz NA, Kim CB, Nork TM, Levin LA, Lucarelli MJ, Kaufman PL, Ver Hoeve JN (2006) Multifocal visual evoked potentials in the anesthetized non-human primate. Curr Eye Res 31:885–893
29. Chauhan BC, Levatte TL, Garnier KL, Tremblay F, Pang IH, Clark AF, Archibald ML (2006) Semiquantitative optic nerve grading scheme for determining axonal loss in experimental optic neuropathy. Invest Ophthalmol Vis Sci 47:634–640
30. Frishman LJ, Saszik S, Harwerth RS, Viswanathan S, Li Y, Smith EL 3rd, Robson JG, Barnes G (2000) Effects of experimental glaucoma in macaques on the multifocal ERG. Multifocal ERG in laser-induced glaucoma. Doc Ophthalmol 100:231–251
31. Hare WA, Ton H, Ruiz G, Feldmann B, Wijono M, WoldeMussie E (2001) Characterization of retinal injury using ERG measures obtained with both conventional and multifocal methods in chronic ocular hypertensive primates. Invest Ophthalmol Vis Sci 42:127–136
32. Hood DC, Frishman LJ, Viswanathan S, Robson JG, Ahmed J (1999) Evidence for a ganglion cell contribution to the primate electroretinogram (ERG): effects of TTX on the multifocal ERG in macaque. Vis Neurosci 16:411–416
33. Hare WA, Ton H (2002) Effects of APB, PDA, and TTX on ERG responses recorded using both multifocal and conventional methods in monkey. Effects of APB, PDA, and TTX on monkey ERG responses. Doc Ophthalmol 105:189–222
34. Heckenlively JR, Tanji T, Logani S (1994) Retrospective study of hyperabnormal (supranormal) electroretinographic responses in 104 patients. Trans Am Ophthalmol Soc 92:217–231; discussion 231-213
35. Feigl B, Haas A, El-Shabrawi Y (2002) Multifocal ERG in multiple evanescent white dot syndrome. Graefes Arch Clin Exp Ophthalmol 240:615–621
36. Ladewig MS, Ladewig K, Guner M, Heidrich H (2005) Prostaglandin E1 infusion therapy in dry age-related macular degeneration. Prostaglandins Leukot Essent Fatty Acids 72:251–256
37. Adachi-Usami E, Mizota A, Ikeda H, Hanawa T, Kimura T (1992) Transient increase of b-wave in the mouse retina after sodium iodate injection. Invest Ophthalmol Vis Sci 33:3109–3113
38. Hood DC, Frishman LJ, Saszik S, Viswanathan S (2002) Retinal origins of the primate multifocal ERG:

implications for the human response. Invest Ophthalmol Vis Sci 43:1673–1685
39. Quigley HA, Nickells RW, Kerrigan LA, Pease ME, Thibault DJ, Zack DJ (1995) Retinal ganglion cell death in experimental glaucoma and after axotomy occurs by apoptosis. Investigative Ophthalmology & Visual Science 36:774–786
40. Raz D, Seeliger MW, Geva AB, Percicot CL, Lambrou GN, Ofri R (2002) The effect of contrast and luminance on mfERG responses in a monkey model of glaucoma. Invest Ophthalmol Vis Sci 43:2027–2035
41. Hare WA, WoldeMussie E, Lai RK, Ton H, Ruiz G, Chun T, Wheeler L (2004) Efficacy and safety of memantine treatment for reduction of changes associated with experimental glaucoma in monkey, I: functional measures. Invest Ophthalmol Vis Sci 45:2625–2639
42. Irifune M, Shimizu T, Nomoto M, Fukuda T (1992) Ketamine-induced anesthesia involves the N-methyl-D-aspartate receptor-channel complex in mice. Brain Res 596:1–9
43. Oye I, Paulsen O, Maurset A (1992) Effects of ketamine on sensory perception: evidence for a role of N-methyl-D-aspartate receptors. J Pharmacol Exp Ther 260:1209–1213
44. Tomlin SL, Jenkins A, Lieb WR, Franks NP (1999) Preparation of barbiturate optical isomers and their effects on GABA(A) receptors. Anesthesiology 90:1714–1722
45. Fortune B, Cull G, Wang L, Van Buskirk EM, Cioffi GA (2002) Factors affecting the use of multifocal electroretinography to monitor function in a primate model of glaucoma. Doc Ophthalmol 105:151–178
46. Vardi N, Duvoisin R, Wu G, Sterling P (2000) Localization of mGluR6 to dendrites of ON bipolar cells in primate retina. J Comp Neurol 423:402–412
47. Mosinger JL, Yazulla S, Studholme KM (1986) GABA-like immunoreactivity in the vertebrate retina: a species comparison. Exp Eye Res 42:631–644
48. Koulen P, SassoePognetto M, Grunert U, Wassle H (1996) Selective clustering of GABA(A) and glycine receptors in the mammalian retina. J Neurosci 16:2127–2140
49. Yazulla S, Studholme KM, Vitorica J, de Blas AL (1989) Immunocytochemical localization of GABAA receptors in goldfish and chicken retinas. J Comp Neurol 280:15–26
50. Vardi N, Sterling P (1994) Subcellular localization of GABAA receptor on bipolar cells in macaque and human retina. Vision Res 34:1235–1246
51. Chao TI, Grosche J, Friedrich KJ, Biedermann B, Francke M, Pannicke T, Reichelt W, Wulst M, Muhle C, Pritz-Hohmeier S, Kuhrt H, Faude F, Drommer W, Kasper M, Buse E, Reichenbach A (1997) Comparative studies on mammalian Muller (retinal glial) cells. J Neurocytol 26:439–454
52. Pannicke T, Biedermann B, Uckermann O, Weick M, Bringmann A, Wolf S, Wiedemann P, Habermann G, Buse E, Reichenbach A (2005) Physiological properties of retinal Muller glial cells from the cynomolgus monkey, Macaca fascicularis–a comparison to human Muller cells. Vision Res 45:1781–1791
53. Luo X, Heidinger V, Picaud S, Lambrou G, Dreyfus H, Sahel J, Hicks D (2001) Selective excitotoxic degeneration of adult pig retinal ganglion cells in vitro. Invest Ophthalmol Vis Sci 42:1096–1106
54. Kremers J, Doelemeyer A, Polska EA, Moret F, Lambert C, Lambrou GN (2008) Multifocal electroretinographical changes in monkeys with experimental ocular hypertension: a longitudinal study. Doc Ophthalmol 117:47–63
55. Raz D, Perlman I, Percicot CL, Lambrou GN, Ofri R (2003) Functional damage to inner and outer retinal cells in experimental glaucoma. Invest Ophthalmol Vis Sci 44:3675–3684
56. Kim CBY, VerHoeve JN, Kaufman PL, Nork TM (2005) Effects of reference electrode location on monopolar-derived multifocal electroretinograms in cynomolgus monkeys. Doc Ophthalmol 111:113–125
57. Heynen H, Wachtmeister L, van Norren D (1985) Origin of the oscillatory potentials in the primate retina. Vision Res 25:1365–1373
58. Ogden TE (1973) The oscillatory waves of the primate electroretinogram. Vision Res 13:1059–1074
59. Wu S, Sutter EE (1995) A topographic study of oscillatory potentials in man. Vis Neurosci 12:1013–1025
60. Fortune B, Cull GA, Burgoyne CF (2008) Relative course of retinal nerve fiber layer birefringence and thickness and retinal function changes after optic nerve transection. Invest Ophthalmol Vis Sci 49:4444–4452
61. Rangaswamy NV, Zhou W, Harwerth RS, Frishman LJ (2006) Effect of experimental glaucoma in primates on oscillatory potentials of the slow-sequence mfERG. Invest Ophthalmol Vis Sci 47:753–767
62. Zhou W, Rangaswamy N, Ktonas P, Frishman LJ (2007) Oscillatory potentials of the slow-sequence multifocal ERG in primates extracted using the Matching Pursuit method. Vision Res 47:2021–2036
63. Mohidin N, Yap MK, Jacobs RJ (1997) The repeatability and variability of the multifocal electroretinogram for four different electrodes. Ophthalmic Physiol Opt 17:530–535
64. Lei Y, Garrahan N, Hermann B, Becker DL, Hernandez MR, Boulton ME, Morgan JE (2008) Quantification of retinal transneuronal degeneration in human glaucoma: a novel multiphoton-DAPI approach. Invest Ophthalmol Vis Sci 49:1940–1945
65. Quigley HA, Dunkelberger GR, Green WR (1989) Retinal ganglion cell atrophy correlated with automated perimetry in human eyes with glaucoma. Am J Ophthalmol 107:453–464
66. Henson DB, Artes PH, Chauhan BC (1999) Diffuse loss of sensitivity in early glaucoma. Invest Ophthalmol Vis Sci 40:3147–3151
67. Kook MS, Lee SU, Sung KR, Tchah H, Kim ST, Kim KR, Kang W (2002) Pattern of retinal nerve fiber layer damage in Korean eyes with normal-tension glaucoma and hemifield visual field defect. Graefes Arch Clin Exp Ophthalmol 240:448–456
68. Mok KH, Lee VW, So KF (2004) Retinal nerve fiber loss in high- and normal-tension glaucoma by optical coherence tomography. Optom Vis Sci 81:369–372
69. Bagga H, Greenfield DS (2004) Quantitative assessment of structural damage in eyes with localized visual field abnormalities. Am J Ophthalmol 137:797–805
70. Glovinsky Y, Quigley HA, Dunkelberger GR (1991) Retinal ganglion cell loss is size dependent in experimental

glaucoma. Investigative Ophthalmology & Visual Science 32:484–491
71. Desatnik H, Quigley HA, Glovinsky Y (1996) Study of central retinal ganglion cell loss in experimental glaucoma in monkey eyes. J Glaucoma 5:46–53
72. Harwerth RS, Carter-Dawson L, Smith EL 3rd, Barnes G, Holt WF, Crawford ML (2004) Neural losses correlated with visual losses in clinical perimetry. Invest Ophthalmol Vis Sci 45:3152–3160